Journal of Spacecraft and Rockets

VOLUME 8 AUGUST 1971 NUMBER 8

Nutation Damping and Vibration Isolation in a Flexibly Coupled Dual-Spin Spacecraft

C. K. CRETCHER*
The Aerospace Corporation, El Segundo, Calif.

AND

D. L. MINGORI†
University of California, Los Angeles, Calif.

As the accuracies required to meet mission objectives become increasingly greater, the suitability of the dual-spin concept rests more and more on its ability to provide a platform free of extraneous motion. This paper is concerned with the possibility of achieving this goal by introducing a flexible, dissipative coupling between the platform and rotor of such a spacecraft. Both analytical and numerical results are presented, and it is shown, for realistic spacecraft designs, throughout that settling times for damping nutation of the order of a few seconds may be obtained, while at the same time, platform vibrations induced by static and dynamic unbalances in the rotor are attenuated by a factor of three or more.

Nomenclature

B,B' = designations of platform and rotor, respectively
$\mathbf{b}$ = $b\mathbf{x}_3$ = vector directed from O to Q
$\mathbf{b}'$ = $b'\mathbf{x}'_3$ = vector directed from Q to O'
$\mathbf{c}$ = vector from system center of mass to O
c_1,c_2 = damping constants [see Eq. (1)]
c = damping constant for symmetric system
C = $c/(I_{33}'\sigma)$ = dimensionless damping constant
$C\alpha$ = $\cos\alpha$ where α is any angle
D = $\{J(1 - J - 1/P) + R(1 - J - J')[R(J + J' - 1/P) - 2J]\}/(1 - 1/P)$
$\mathbf{F}$ = external force applied to B' at Q
$\mathbf{h}$ = $\sum_{i=1}^{3} h_i\mathbf{x}_i$ = system angular momentum vector
H = magnitude of $\mathbf{h}$
$\bar{\mathbf{I}}$ = $\sum_{i=1}^{3} I_{ii}\mathbf{x}_i\mathbf{x}_i$ = centroidal moment of inertia dyadic for the platform
$\bar{\mathbf{I}}'$ = $\sum_{i=1}^{3} I_{ii}'\mathbf{y}_i\mathbf{y}_i$ = centroidal moment of inertia dyadic for the rotor
I_T = $I_{11} + I_{11}' + (b + b')^2$
J = I_{11}/I_T
J' = I_{11}'/I_T
$\bar{J}$ = J if $R = 0$; $(1 - J')$ if $R = 1$
k_1,k_2 = spring constants [see Eq. (1)]
k = spring constant for symmetric system
K = $kI_T/(I_{33}'\sigma)^2$ = dimensionless spring constant
m,m' = masses of B and B', respectively
O,O^* = actual mass centers of B and B', respectively
O' = point fixed in B' near O^*
P = I_T/I_{33}'
Q = center of flexible coupling
R = $b/(b + b')$
S^* = root of Eq. (25) nearest the imaginary axis
$S\alpha$ = $\sin\alpha$ where α is any angle
T_s = $I_T/(I_{33}'\sigma ReS^*)$ = dimensionless settling time
T_1,T_2 = restoring torque components for $\mathbf{x}_1$ and $\mathbf{x}_3' \times \mathbf{x}_1$ directions, respectively
$\mathbf{T}_c$ = pure couple applied to B by B'
$\mathbf{u}$ = $\sum_{i=1}^{3} u_i\mathbf{x}_i$ = inertial angular velocity of B
$\mathbf{v}$ = $\sum_{i=1}^{3} v_i\mathbf{y}_i$ = inertial angular velocity of B'
w_1,w_2 = see Eq. (18)
X_1,X_2,X_3 = centroidal principal axes for the platform
X_3' = axis fixed in B'; nominally the symmetry axis
$\mathbf{x}_1,\mathbf{x}_2,\mathbf{x}_3$ = unit vectors directed along X_1, X_2, X_3, respectively
$\mathbf{x}_3'$ = unit vector along X_3'
Y_1,Y_2,Y_3 = centroidal principal axes of B'
$\mathbf{y}_1,\mathbf{y}_2,\mathbf{y}_3$ = unit vectors along Y_1, Y_2, and Y_3, respectively
γ = $C/(PD)$
δ_1 = $\mu(b + b')(b'\phi_2 + \epsilon_1)/I_T$
δ_2 = $\mu(b + b')(-b'\phi_1 + \epsilon_2)/I_T$
$\boldsymbol{\epsilon}$ = $\sum_{i=1}^{3} \epsilon_i\mathbf{y}_i$ = vector directed from O' to O^*
θ_1,θ_2 = gimbal angles
ω = $K/(P^2D)$
μ = $mm'/(m + m')$ = "reduced mass"
ρ = isolation factor
σ = relative rotor speed (assumed constant)
τ = $1/ReS^*$ = dimensionless settling time

Received November 20, 1970; revision received March 12, 1971.

* Staff Engineer, Defense Navigation Satellite Systems Office; formerly graduate student, School of Engineering and Applied Science, University of California, Los Angeles, Calif.

† Assistant Professor, School of Engineering and Applied Science. Member AIAA.

ϕ_1,ϕ_2 = angles for describing the orientation of X_3' relative to Y_1, Y_2, Y_3 (Fig. 2 describes these angles when θ_1, θ_2, X_1, X_2 and X_3 are relabeled as ϕ_1, ϕ_2, Y_1, Y_2 and Y_3, respectively). Thus ϕ_1 is a rotation about y_1 and ϕ_2 is a rotation about $\mathbf{x}_3' \times \mathbf{y}_1$

Φ = coning angle, i.e., angle between $\mathbf{x}_3$ and $\mathbf{h}$

Introduction

DUAL-SPIN spacecraft, i.e., spacecraft consisting of two primary sections that nominally rotate at different rates in inertial space, have received considerable attention recently because of their ability to satisfy certain mission requirements more readily than vehicles that either spin as a unit or employ purely reaction jet or reaction wheel control systems.[1,2] Typically, such spacecraft are designed to maintain a "despun platform" in a desired orientation in space, gyroscopic stabilization being provided by a "rotor." Two obstacles to the achievement of this goal are nutational motions resulting from small external disturbances or internal dissipation, and wobble resulting from static and/or dynamic unbalances in the rotor. This paper deals with the possibility of overcoming these obstacles by introducing a flexible coupling between the rotor and the platform.‡

The coupling considered is modeled as a two-degree-of-freedom universal joint which produces linear elastic and viscous restoring torques when deformed from its nominal configuration. It is shown that such a device can attenuate nutational or coning motion resulting from a discrete disturbance by a factor of $1/e$ in a matter of a few seconds, and reduce wobble to a degree limited only by considerations of physical realizability and the desire to retain a given level of performance with respect to the attenuation of nutation. Numerical studies employing typical spacecraft parameters demonstrate that it is possible to devise realistic coupling designs that effectively accomplish both of these tasks simultaneously.

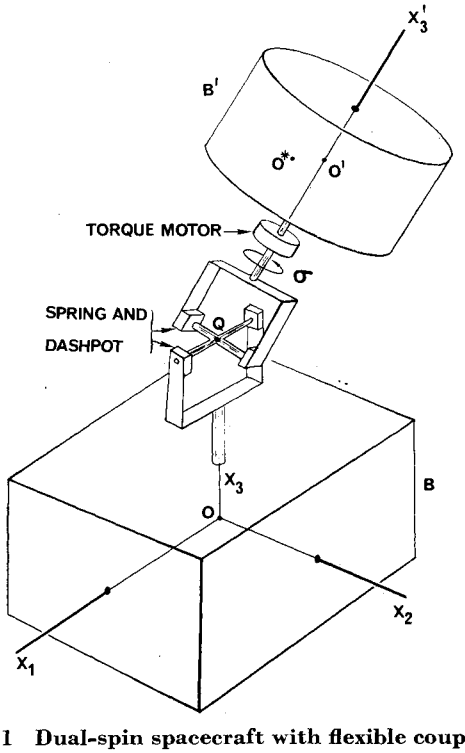

Fig. 1 Dual-spin spacecraft with flexible coupling.

‡ After substantial progress had been made in this investigation, it was discovered that a similar system was studied by Rubin and Swanson of the Hughes Aircraft Company. Their work has not appeared in the open literature, but it has been documented in Ref. 3, an internal company report.

Idealized Spacecraft Model

An idealized model of a dual-spin spacecraft with a flexible coupling is depicted in Fig. 1. The axes X_1, X_2 and X_3 are centroidal principal axes for the platform B, X_3' is an axis fixed in the rotor B', and O' is a point fixed on X_3'. Except for small unbalances which are unavoidable in construction, X_3' may be considered the symmetry axis and O' the mass center of R. A set of unit vectors $\mathbf{x}_1$, $\mathbf{x}_2$, $\mathbf{x}_3$ and $\mathbf{x}_3'$ directed along X_1, X_2, X_3 and X_3', respectively, will be useful in the following development.

The flexible universal joint permits rotations of X_3' relative to B which may be described in terms of a rotation of amount θ_1 about an axis parallel to X_1 and θ_2 about an axis perpendicular to both X_1 and X_3' (see Fig. 2). Such rotations are resisted by torques of the form

$$T_i = k_i\theta_i + c_i\dot{\theta}_i; \quad i = 1,2 \tag{1}$$

where T_1 and T_2 act on B, T_1 being directed along $\mathbf{x}_1$ and T_2 along $\mathbf{x}_3' \times \mathbf{x}_1$. It is assumed that when the coupling is undeformed, X_3 and X_3' coincide. The k_i's and c_i's are spring and damping constants, respectively.

A torque motor is used to maintain the desired rotational speed between B' and the portion of the flexible joint nearest B'. It is important to locate this motor on the side of the coupling nearest the rotor in order that dissipation in the coupling be associated with the platform. This is required to insure stability as discussed in Refs. 1 and 2. Although the motor may also be used to control platform pointing in actual applications, the assumption of a constant relative speed σ is employed here to simplify the analytical development.

A realistic model of a dual-spin spacecraft would include the effects of passive energy dissipation on both the rotor and the platform as these have been shown to have a profound influence on stability and performance.[1,2,4] It will be demonstrated, however, that a properly designed mechanism of the type under consideration is so effective in attentuating nutation and wobble, that the decision to ignore these other sources of dissipation seems quite reasonable.

Equations of Motion

Three of the five scalar dynamical equations required for describing the motion of this system may be obtained by applying the angular momentum principle to the entire system. Assuming that no external torques act, the vector representation of these equations assumes the form

$$\bar{\mathbf{I}}\cdot\dot{\mathbf{u}} + \mathbf{u} \times (\bar{\mathbf{I}}\cdot\mathbf{u}) + \bar{\mathbf{I}}'\cdot\dot{\mathbf{v}} + \mathbf{v} \times (\bar{\mathbf{I}}'\cdot\mathbf{v}) + \mu(\mathbf{b} + \mathbf{b}' + \boldsymbol{\varepsilon}) \times \{\dot{\mathbf{u}} \times \mathbf{b} + \mathbf{u} \times (\mathbf{u} \times \mathbf{b}) + \dot{\mathbf{v}} \times (\mathbf{b}' + \boldsymbol{\varepsilon}) + \mathbf{v} \times [\mathbf{v} \times (\mathbf{b}' + \boldsymbol{\varepsilon})]\} = 0 \tag{2}$$

where a dot over a vector indicates differentiation in an inertial reference frame.

Two additional scalar equations may be obtained by applying the angular momentum principle to the platform alone. Of course, forces and torques applied to the platform at the

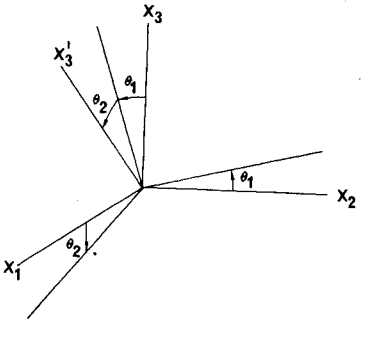

Fig. 2 Orientation angles.

coupling must be considered as external in this part of the development. Thus the relevant vector equation becomes

$$\bar{\mathbf{I}}\cdot\dot{\mathbf{u}} + \mathbf{u} \times (\bar{\mathbf{I}} \times \mathbf{u}) = \mathbf{T}_c + \mathbf{b} \times \mathbf{F} \tag{3}$$

where $\mathbf{T}_c$ and $\mathbf{F}$ form an equivalent force system for all external forces applied to B, $\mathbf{T}_c$ being a pure couple and $\mathbf{F}$ a force applied at point Q. $\mathbf{F}$ may be expressed in terms of the quantities introduced earlier by means of the center of mass theorem which states that

$$\mathbf{F} = m\ddot{\mathbf{c}} \tag{4}$$

In this equation, $\mathbf{c}$ is a vector from the system center of mass (fixed in inertial space) to O. From the definition of mass center

$$m\mathbf{c} + m'(\mathbf{c} + \mathbf{b} + \mathbf{b}' + \boldsymbol{\varepsilon}) = 0 \tag{5}$$

Substitution of Eq. (5) into Eq. (4) yields

$$\mathbf{F} = -\mu(\ddot{\mathbf{b}} + \ddot{\mathbf{b}}' + \ddot{\boldsymbol{\varepsilon}}) \tag{6}$$

By next substituting Eq. (6) into Eq. (3) and then taking the dot product of the resulting equation once with $\mathbf{x}_1$ and once with a unit vector $(\mathbf{x}_2 C\theta_1 + \mathbf{x}_3 S\theta_1)$ which is parallel to $\mathbf{x}_3' \times \mathbf{x}_1$ (these dot multiplications eliminate constraint torques in $\mathbf{T}_c$), the following required scalar equations are obtained

$$\mathbf{x}_1\cdot[\bar{\mathbf{I}}\cdot\dot{\mathbf{u}} + \mathbf{u} \times (\bar{\mathbf{I}} \times \mathbf{u}) + \mu\mathbf{b} \times (\ddot{\mathbf{b}} + \ddot{\mathbf{b}}' + \ddot{\boldsymbol{\varepsilon}})] - k_1\theta_1 - c_1\dot{\theta}_1 = 0 \tag{7}$$

$$(\mathbf{x}_2 C\theta_1 + \mathbf{x}_3 S\theta_1)\cdot[\bar{\mathbf{I}}\cdot\dot{\mathbf{u}} + \mathbf{u} \times (\bar{\mathbf{I}} \times \mathbf{u}) + \mu\mathbf{b} \times (\ddot{\mathbf{b}} + \ddot{\mathbf{b}}' + \ddot{\boldsymbol{\varepsilon}})] - k_2\theta_2 - c_2\dot{\theta}_2 = 0 \tag{8}$$

When all of the indicated vector operations are performed, Eqs. (3, 7 and 8) may be expressed as five scalar equations in the eight dependent variables $u_1, u_2, u_3, v_1, v_2, v_3, \theta_1$ and θ_2. To form a complete set of equations, three kinematical relationships must be supplied. These are obtained by considering the relationship between the inertial angular velocities of B and B'. Hence

$$\mathbf{v} = \mathbf{u} + \dot{\theta}_1\mathbf{x}_1 + \dot{\theta}_2(\mathbf{x}_2 C\theta_1 + \mathbf{x}_3 S\theta_1) + \sigma\mathbf{x}_3' \tag{9}$$

This vector equation provides the three desired scalar equations.

The nonlinear scalar equations obtained from Eqs. (3) and (7–9) were written out and programed on a digital computer so that the results of investigations based on simplified equations could be checked. Although somewhat tedious, this exercise is straightforward and will not, therefore, be pursued further here. Instead, we shall turn our attention to a set of linearized equations obtained from the full nonlinear equations by assuming that $u_1, u_2, u_3, v_1, v_2, v_3 - \sigma, \theta_1, \theta_2, \varphi_1, \varphi_2, \epsilon_1, \epsilon_2$ and ϵ_3 remain small so that all nonlinear terms in these quantities and their time derivatives may be ignored. It should be noted that not all of the quantities assumed to be small are dependent variables. Some are constants resulting from manufacturing imperfections. The latter group leads to periodic forcing terms in the governing equations.

After carrying out this linearization, the following set of equations is obtained.

System Equations

$$I_{11}\dot{u}_1 + I_{11}'\dot{v}_1 C\sigma t - I_{22}'\dot{v}_2 S\sigma t - (I_{22}' - I_{33}')\sigma v_2 C\sigma t - (I_{11}' - I_{33}')\sigma v_1 S\sigma t + \mu(b + b')\{b\dot{u}_1 + b'(\dot{v}_1 C\sigma t - \dot{v}_2 S\sigma t) - b'\sigma(v_1 S\sigma t + v_2 C\sigma t) + \sigma^2[(b'\varphi_2 + \epsilon_1)S\sigma t + (-b'\varphi_1 + \epsilon_2)C\sigma t]\} = 0 \tag{10}$$

$$I_{22}\dot{u}_2 + I_{11}'\dot{v}_1 S\sigma t + I_{22}'\dot{v}_2 C\sigma t - (I_{33}' - I_{11}')\sigma v_1 C\sigma t + (I_{33}' - I_{22}')\sigma v_2 S\sigma t + \mu(b + b')\{b\dot{u}_2 + b'(\dot{v}_1 S\sigma t + \dot{v}_2 C\sigma t) + b'\sigma(v_1 C\sigma t - v_2 S\sigma t) + \sigma^2[-(b'\varphi_2 + \epsilon_1)C\sigma t + (-b'\varphi_1 + \epsilon_2)S\sigma t]\} = 0 \tag{11}$$

$$I_{33}\dot{u}_3 + I_{33}'\dot{v}_3 = 0 \tag{12}$$

Platform Equations

$$I_{11}\dot{u}_1 - k_1\theta_1 - c_1\dot{\theta}_1 + \mu b\{b\dot{u}_1 + b'(\dot{v}_1 C\sigma t - \dot{v}_2 S\sigma t) - b'\sigma(v_1 S\sigma t + v_2 C\sigma t) + \sigma^2[(b'\varphi_2 + \epsilon_1)S\sigma t + (-b'\varphi_1 + \epsilon_2)C\sigma t]\} = 0 \tag{13}$$

$$I_{22}\dot{u}_2 - k_2\theta_2 - c_2\dot{\theta}_2 + \mu b\{b\dot{u}_2 + b'(\dot{v}_1 S\sigma t + \dot{v}_2 C\sigma t) + b'\sigma(v_1 C\sigma t - v_2 S\sigma t) + \sigma^2[-(b'\varphi_2 + \epsilon_1)C\sigma t + (-b'\varphi_1 + \epsilon_2)S\sigma t] = 0\} \tag{14}$$

Kinematics

$$u_1 + \dot{\theta}_1 = v_1 C\sigma t - v_2 S\sigma t + \sigma(\varphi_1 S\sigma t + \varphi_2 C\sigma t) \tag{15}$$

$$u_2 + \dot{\theta}_2 = v_1 S\sigma t + v_2 C\sigma t + \sigma(-\varphi_1 C\sigma t + \varphi_2 S\sigma t) \tag{16}$$

$$u_3 + \sigma = v_3 \tag{17}$$

These equations may be expressed in a more convenient form by a) eliminating Eqs. (12) and (17) from consideration by noting that these equations are uncoupled from the remaining equations and serve only to reinforce the assumption that u_3 and $v_3 - \sigma$ remain small; b) introducing two new dependent variables w_1 and w_2 defined as

$$w_1 = v_1 C\sigma t - v_2 S\sigma t; \quad w_2 = v_1 S\sigma t + v_2 C\sigma t \tag{18}$$

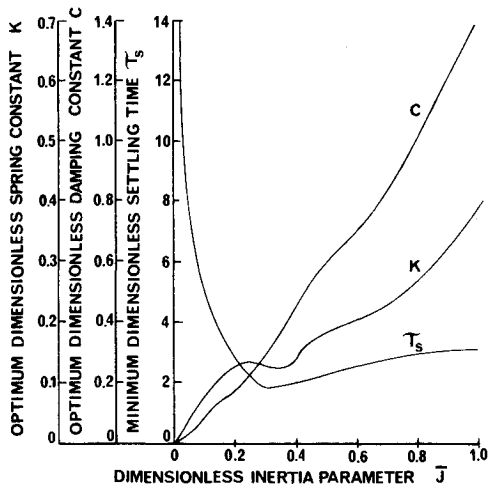

Fig. 3 Nutation damping: optimum system parameters and settling times.

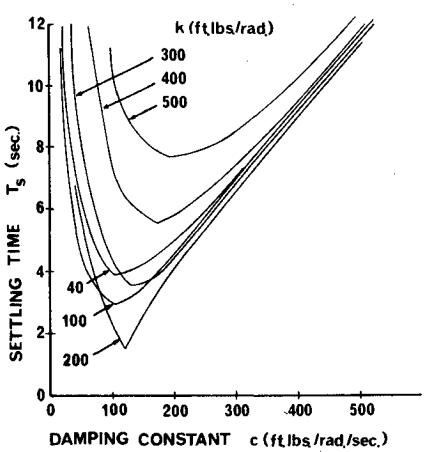

Fig. 4 Nutation damping: T_s vs c and k for a symmetric system with $R = 0$.

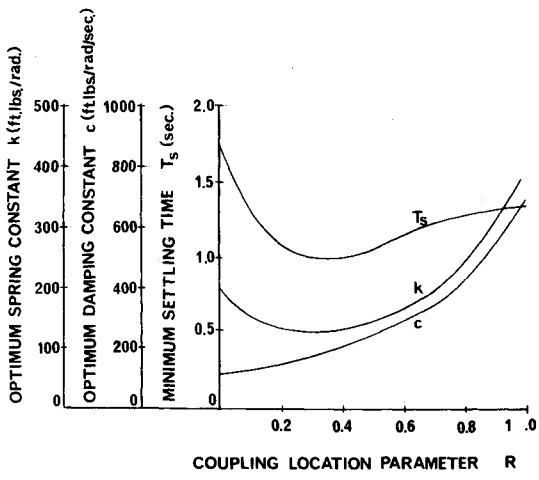

Fig. 5 Nutation damping: variation of T_s with gimbal location.

and c) assuming that the difference $I_{11}' - I_{22}'$ is a small number Δ which may be ignored when multiplied by one of the quantities assumed small in obtaining Eqs. (10–17) from Eqs. (3) and (7–9). After incorporating these definitions, observations and assumptions, Eqs. (10–17) reduce to the following set of equations:

$$[I_{11} + \mu(b + b')b]\dot{u}_1 + [I_{11}' + \mu(b + b')b']\dot{w}_1 + I_{33}'\sigma w_2 = -\mu(b + b')\sigma^2[(b'\varphi_2 + \epsilon_1)S\sigma t + (-b'\varphi_1 + \epsilon_2)C\sigma t] \quad (19)$$

$$[I_{22} + \mu(b + b')b]\dot{u}_2 + [I_{11}' + \mu(b + b')b']\dot{w}_2 - I_{33}'\sigma w_1 = -\mu(b + b')\sigma^2[-(b'\varphi_2 + \epsilon_1)C\sigma t + (-b'\varphi_1 + \epsilon_2)S\sigma t] \quad (20)$$

$$[I_{11} + \mu b^2]\dot{u}_1 + \mu bb'\dot{w}_1 - c_1\dot{\theta}_1 - k_1\theta_1 = -\mu b\sigma^2[(b'\varphi_2 + \epsilon_1)S\sigma t + (-b'\varphi_1 + \epsilon_2)C\sigma t] \quad (21)$$

$$[I_{22} + \mu b^2]\dot{u}_2 + \mu bb'\dot{w}_2 - c_2\dot{\theta}_2 - k_2\theta_2 = -\mu b\sigma^2[-(b'\varphi_2 + \epsilon_1)C\sigma t + (-b'\varphi_1 + \epsilon_2)S\sigma t] \quad (22)$$

$$u_1 + \dot{\theta}_1 - w_1 = \sigma(\varphi_1 S\sigma t + \varphi_2 C\sigma t) \quad (23)$$

$$u_2 + \dot{\theta}_2 - w_2 = \sigma(-\varphi_1 C\sigma t + \varphi_2 S\sigma t) \quad (24)$$

Equations (19–24) are now in a form useful for the study of both the decay of free coning or nutation, and the reduction of wobble due to unbalances.

Nutation Damping

The rate at which transient nutational motion decays can be estimated by examining the roots of the characteristic equation of the homogeneous part of Eqs. (19–24). In order to simplify the development, it will be assumed initially that the platform is symmetric ($I_{11} = I_{22}$), $c_1 = c_2$, and $k_1 = k_2$. The consequences of removing these restrictions are discussed briefly at the end of this section.

For the symmetric system, the characteristic equation may be expressed most compactly in complex form. With coefficients written in terms of symbols defined in the nomenclature, this equation becomes

$$S^3\{JJ' + (1 - J - J')[J(1 - R)^2 + J'R^2]\} + S^2\{C - j[J + (1 - J - J')R^2]\} + S\{K - jC\} - jK = 0 \quad (25)$$

where $j = (-1)^{1/2}$. A useful index of the rate at which transient nutational motions decay is the settling time T_s defined as the time required for all transient oscillations to decay by a factor of $1/e$. After the roots of Eq. (25) are found (it can be shown that these roots always lie in the left half of the complex plane), T_s may be calculated from the expression

$$T_s = |I_T/(I_{33}'\sigma ReS^*)| \quad (26)$$

where S^* is the root of Eq. (25) nearest the imaginary axis. Normally it is desired that T_s be made as small as possible. The effectiveness of the system under consideration in achieving this goal is examined next.

If the flexible coupling is located at the center of mass of either body ($R = 0$ or 1), the vehicle mass properties may be characterized by a single variable $\bar{J}$ defined as

$$\bar{J} = \begin{cases} J & \text{if } R = 0 \\ 1 - J' & \text{if } R = 1 \end{cases} \quad (27)$$

In either case, Eq. (25) reduces to

$$S^3\bar{J}(1 - \bar{J}) + S^2(C - j\bar{J}) + S(K - jC) - jK = 0 \quad (28)$$

For purposes of calculating roots numerically this third-degree polynomial with complex coefficients was transformed into an equivalent sixth-degree polynomial with real coefficients, and this result was programed on a digital computer. Then $\bar{J}$ was allowed to vary over its entire range of zero to one, and, for each value of $\bar{J}$, the values of K and C that minimized the system settling time were determined by a straightforward two-parameter numerical search. The results of carrying out this procedure are displayed in Fig. 3, where a dimensionless settling time $\tau_s \equiv |1/ReS^*|$ has been introduced to make it unnecessary to specify a value for $I_T/(I_{33}'\sigma)$ [see Eq. (26)], thus retaining greater generality.

It is meaningful to consider the results of Fig. 3 in the light of certain design criteria associated with conventional nutation dampers. The selection of spring constants for such devices is often guided by the notion that the damper natural frequency should be at or near the so-called "nutation frequency," a quantity typically calculated by analyzing the free coning motion of the vehicle while ignoring vehicle flexibility.[5] This design philosophy is likely to be unsatisfactory for the present system because of the considerable effect of the flexible coupling on the overall vehicle motion. Not only is the calculation of a nutation frequency from a model neglecting flexibility inappropriate, but even if an equivalent quantity could be found, there is no readily available expression that may be identified as the "damper natural frequency."

In spite of its possible shortcoming as a design tool, a procedure based on that just discussed is worth applying to the present system for comparison. Suppose one a) calculates the nutation frequency as seen in the platform by analyzing the free motions of the dual-spin system without a flexible coupling, b) designates as the damper natural frequency the frequency at which the platform would freely oscillate if the rotor axis were held fixed in inertial space, c) selects the dimensionless spring parameter K in such a way that the damper natural frequency found in b equals the nutation frequency found in a, and d) computes settling times as C is allowed to vary and K is held fixed at the value found in c. The "tuned" K and the corresponding minimum settling time found in this way are generally somewhat larger than the values indicated in Fig. 3. Consider, for example, a spacecraft for which

$$I_{11} = I_{22} = I_{33} = 64 \text{ slug ft}^2$$

$$I_{11}' = I_{22}' = 155 \text{ slug ft}^2; \quad I_{33}' = 136 \text{ slug ft}^2$$

$$m = 17 \text{ slug}; \quad m' = 20 \text{ slug}$$

$$b + b' = 4.54 \text{ ft}; \quad \sigma = 6.28 \text{ rad/sec} \quad (29)$$

These mass properties and spin rate closely approximate those of the Intelsat IV spacecraft. The value of $\bar{J}$ for this system is 0.156. If the flexible connection is located at the platform mass center ($R = 0$), then the tuned K and the corresponding minimum τ_s are 0.156 and 6.7, respectively, while the corresponding optimum values from Fig. 3 are 0.11 and 3.55. To give some physical significance to the damping parameter C, it may be mentioned that the curve in Fig. 3 giving C as a function of $\bar{J}$ closely approximates one which whould be ob-

tained if C were required to critically damp free oscillations of the platform when the rotor axis is inertially fixed.

The possibility of obtaining low settling times with realistic spring and damping constants is explored in Fig. 4 for the system described in Eq. (29) with $k_1 = k_2 = k$, $c_1 = c_2 = c$, and $R = 0$ (i.e., $b = 0, b' = 4.54$ ft). The curves shown were obtained by numerical search involving calculation of the roots of the characteristic polynomial and the use of Eq. (26). They indicate that a T_s of only 1.65 sec is achievable with $k = 200$ ft-lb/rad and $c = 124$ lb/rad/sec. Although a coupling built to these specifications would no doubt have to be caged during launch, it does not seem to represent a significant obstacle in terms of physical realizability. The achievable T_s is extremely small when compared with settling times of between 5 and 30 min provided by conventional nutation dampers.

The effect of varying the coupling location is explored in Fig. 5. Here k and c were allowed to vary and minimum values of T_s were computed for $0 \leq R \leq 1$. Although there is some variation in the optimum k, c and T_s, gimbal location does not seem to be a critical parameter.

Because some dual-spin spacecraft designs do not have axisymmetric platforms, a numerical study was carried out to assess the effects of platform asymmetry and the desirability of employing different spring and damping constants in each of the two coupling axes of such a system. The scope of the study was necessarily limited, and the results were not comprehensive, but it appears that: a) if the transverse moments of inertia of the platform of an initially symmetric spacecraft are varied with their product held constant, the minimum T_s that can be achieved with symmetric spring and damping constants does not change significantly; and b) the improvement afforded by employing different spring and damping constants in the two axes of the coupling is not marked.

Vibration Isolation

Returning now to the full set of linearized equations including forcing terms [Eqs. (19–24)], we shall examine the possibility of reducing oscillations of the platform arising from unbalances in the rotor. After first defining the coning angle Φ as the angle between X_3 and the system angular momentum vector, a useful index of performance ρ called the "isolation factor" may be defined as the ratio of the amplitude of Φ for the system with a flexible coupling to the amplitude of Φ for the same system with a rigid connecting shaft. The evaluation of Φ and hence of ρ will be based on the steady-state solution of Eqs. (19–24).

Since Eqs. (19–24) are linear, constant-coefficient equations with sinusoidal forcing functions, their solution will have the form

$$x = A_c \cos\sigma t + A_s \sin\sigma t \tag{30}$$

where A_c and A_s are 6×1 constant matrices, and

$$x \equiv [u_1 u_2 w_1 w_2 \theta_1 \theta_2]^T \tag{31}$$

After writing Eqs. (19–24) in matrix forms as

$$\overset{6\times6}{M}\dot{x} + \overset{6\times6}{N}\,x = \overset{6\times1}{F_c}\cos\sigma t + \overset{6\times1}{F_s}\sin\sigma t \tag{32}$$

it can be shown that

$$A_c = -(NM^{-1}N + \sigma^2 M)^{-1}(NM^{-1}F_c + \sigma F_s) \tag{33}$$

and

$$A_s = -(NM^{-1}N + \sigma^2 M)^{-1}(NM^{-1}F_s - \sigma F_c) \tag{34}$$

To obtain an expression for Φ, the system angular momentum vector $\mathbf{h}$ is first expressed in terms of $\mathbf{x}_1$, $\mathbf{x}_2$ and $\mathbf{x}_3$. For small x and small unbalances

$$\begin{aligned}\mathbf{h} &= h_1\mathbf{x}_1 + h_2\mathbf{x}_2 + h_3\mathbf{x}_3 \\ &= \{[I_{11} + \mu(b + b')b]u_1 + [I_{11}' + \mu(b + b')b']w_1 + \\ &\quad I_{33}'\sigma\theta_2 + [I_{33}' - \mu(b + b')b']\sigma(\varphi_1 S\sigma t + \varphi_2 C\sigma t) + \\ &\quad \mu(b + b')\sigma(\epsilon_2 S\sigma t - \epsilon_1 C\sigma t)\}\mathbf{x}_1 + \{[I_{22} + \mu(b + b')b]u_2 + \\ &\quad [I_{11}' + \mu(b + b')b']w_2 - I_{33}'\sigma\theta_1 + \\ &\quad [I_{33}' - \mu(b + b')b']\sigma(-\varphi_1 C\sigma t + \varphi_2 S\sigma t) - \\ &\quad \mu(b + b')\sigma(\epsilon_1 S\sigma t + \epsilon_2 C\sigma t)\}\mathbf{x}_2 + \\ &\quad \{I_{33}u_3 + I_{33}'(v_3 - \sigma) + I_{33}'\sigma)\}\mathbf{x}_3 \end{aligned} \tag{35}$$

Then

$$\Phi = |\mathbf{x}_3 \times (\mathbf{h}/|\mathbf{h}|)| \doteq (h_1^2 + h_2^2)^{1/2}/(I_{33}'\sigma) \tag{36}$$

Φ may be calculated by first finding x using Eqs. (19–24) and (30–34), and then using this result together with Eq. (35) to determine h_1 and h_2 for substitution into Eq. (36). The isolation factor is then obtained by dividing the amplitude of Φ for the system of interest by the amplitude of Φ for the same system with the c's and k's assigned infinite (or at least very large) values. Although a computer is normally required to accomplish this task, it is again possible to make some progress analytically by employing the assumption that the system is symmetric.

For the symmetric system ($I_{11} = I_{22}$, $k_1 = k_2 = k$, $c_1 = c_2 = c$), a complex formulation is advantageous. Let

$$z \equiv \begin{Bmatrix} u_1 + ju_2 \\ w_1 + jw_2 \\ \theta_1 + j\theta_2 \end{Bmatrix}, \quad \bar{F} \equiv \begin{Bmatrix} F_{c1} - jF_{s1} \\ F_{c3} - jF_{s3} \\ F_{c5} - jF_{s5} \end{Bmatrix} \tag{37}$$

$$\bar{M} \equiv \begin{bmatrix} M_{11} & M_{13} & 0 \\ M_{31} & M_{33} & M_{35} \\ 0 & 0 & M_{55} \end{bmatrix}, \quad \bar{N} \equiv \begin{bmatrix} 0 & -jN_{14} & 0 \\ 0 & 0 & N_{35} \\ N_{51} & N_{53} & 0 \end{bmatrix} \tag{38}$$

where the elements of these matrices are taken from Eqs. (19–24) and (32). The governing equations can then be written

$$\bar{M}\dot{z} + \bar{N}z = Fe^{j\sigma t} \tag{39}$$

and the steady-state solution becomes

$$z = [j\sigma\bar{M} + \bar{N}]^{-1}Fe^{j\sigma t} \tag{40}$$

The introduction of a complex quantity $\bar{h} \equiv h_1 + jh_2$ permits Φ to be expressed in the form

$$\Phi = (\bar{h}\bar{h}^*)^{1/2}/(I_{33}'\sigma) \tag{41}$$

where $\bar{h}^*$ is the complex conjugate of $\bar{h}$. From the angular momentum principle,

$$\begin{aligned}(d/dt)(h_1\mathbf{x}_1 + h_2\mathbf{x}_2 + h_3\mathbf{x}_3) &\doteq (\dot{h}_1 + u_2 h_3)\mathbf{x}_1 + \\ &\quad (\dot{h}_2 - u_1 h_3)\mathbf{x}_2 + (\dot{h}_3)\mathbf{x}_3 = 0 \end{aligned} \tag{42}$$

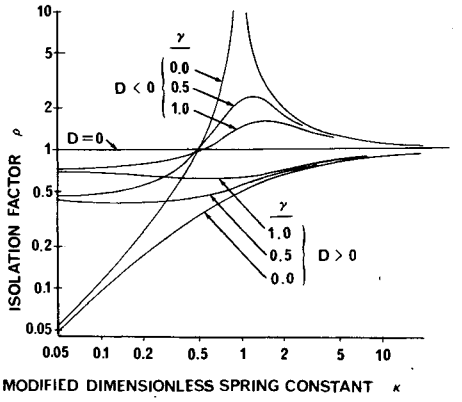

Fig. 6 Vibration isolation: ρ as a function of κ, γ and D.

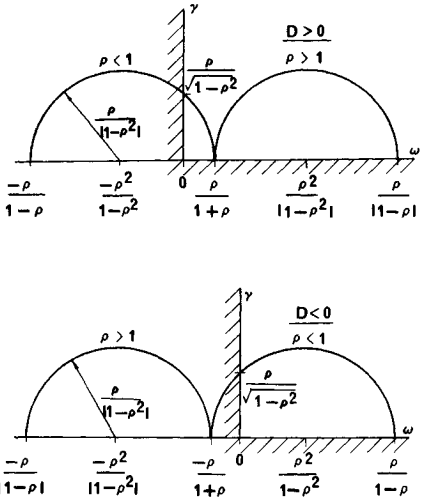

Fig. 7 Vibration isolation: construction of γ vs κ curves.

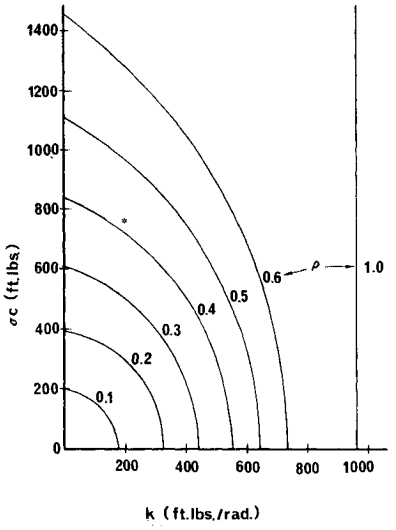

Fig. 8 Vibration isolation: c vs k curves.

Hence,

$$\dot{h}_1 = -u_2 h_3; \quad \dot{h}_2 = u_1 h_3 \tag{43}$$

Since we are dealing with linearized equations, $\bar{h}$ must have the form $\bar{h} = He^{j\sigma t}$ from which it follows that

$$\dot{\bar{h}} = \dot{h}_1 + j\dot{h}_2 = j\sigma H e^{j\sigma t} = jh_3(u_1 + ju_2) = jh_3 z_1 \tag{44}$$

[see Eqs. (37) and (43)]. Thus

$$\bar{h} = h_1 + jh_2 = He^{j\sigma t} = h_3 z_1/\sigma \tag{45}$$

Upon substitution from Eq. (45), Eq. (41) becomes

$$\Phi = (z_1 z_1^*)^{1/2}/\sigma \tag{46}$$

This equation is a convenient one for calculating Φ once z_1 is determined from Eq. (40).

To find the isolation factor ρ, the magnitude of Φ for the system of interest is divided by the magnitude of Φ for the same system except with k and c infinite. After a considerable amount of algebra, Eqs. (19–24, 32, 37, 38, 40, and 46) may be combined to yield

$$\rho = \left\| \frac{K + jPC - \dfrac{P^2R(J' - 1/P)(\delta_1 + j\delta_2)}{(\delta_1 + j\delta_2) - j[1 - J - R(1 - J - J') - 1/P](\varphi_1 + j\varphi_2)}}{K + jPC - P^2D} \right\| \tag{47}$$

The double vertical lines are used to denote the magnitude of the complex quantity inside. Note from the definition of D that if P equals one, ρ becomes zero. This condition represents a situation in which the steady-state response of the rigid system is unbounded, and therefore the suggestion that isolation is complete is misleading.

Since the values of the unbalance terms δ_1, δ_2, φ_1 and φ_2 are generally unknown, it is desirable that ρ be independent of these quantities, which is possible if any of the following condtions hold: a) $R = 0$—the coupling is at the platform mass center; b) $J'P = 1$—the rotor is inertially spherical; or c) $P[1 - J - R(1 - J - J')] = 1 \Leftrightarrow I_{11}' + \mu(b + b')b' = I_{33}'$. Note that condition c can be satisfied by proper coupling location.

If either a or b is satisfied, the isolation factor reduces to

$$\rho = \left\| \frac{K + jPC}{K + jPC - P^2D} \right\| \tag{48}$$

while if c is satisfied

$$\rho = \left\| \frac{K + jPC - P^2R(J' - 1/P)}{K + jPC - P^2D} \right\| \tag{49}$$

To illustrate the effectiveness of the isolation system, attention will be focused on Eq. (48). By introducing $\kappa \equiv K/P^2D$ and $\gamma \equiv C/PD$ this equation may be expressed in a form more suitable for graphical representation as

$$\rho = \left\{ \frac{\kappa^2 + \gamma^2}{[\kappa - \text{sgn}(D)]^2 + \gamma^2} \right\}^{1/2} \tag{50}$$

Figure 6 displays ρ vs κ for several values of γ and D. These curves demonstrate that unless D is zero, isolation is always possible for sufficiently small k and c. Furthermore, if D is positive, some isolation occurs regardless of the values of k and c.

Figure 7 shows γ vs κ with ρ as a parameter. The curves are arcs of circles of radius $\rho/(1 - \rho^2)$ whose centers lie at

$$\kappa = -\text{sgn}(D)[\rho^2/(1 - \rho^2)]; \quad \gamma = 0 \tag{51}$$

This construction is a convenient way of examining the relationships among κ, γ, and ρ without extensive computations.

To illustrate more clearly the relationship between ρ, k, and c, the spacecraft described by Eq. (29) is again investigated. Assuming the coupling to be located at the platform mass center, D becomes 0.119, and the curves of Fig. 8 describe the relationship between c and k for several values of ρ. (In this figure, σc is used as the ordinate to preserve the circularity of the curves.) These curves indicate that a high degree of isolation is possible over a fairly wide range of coupling parameters.

As before, the possible effects of changing the coupling location and/or allowing the platform to be asymmetrical were explored briefly. Although these investigations were not extensive, there was no indication that modifications of this kind would have a significant impact on the results that have been presented.

Concluding Discussion

There are at least two reasons for incorporating a flexible coupling into a dual-spin spacecraft: 1) to rapidly attenuate transient nutational or coning motion; and 2) to reduce platform wobble resulting from rotor unbalances. The results presented so far demonstrate that either of these goals can be attained for properly designed systems, but we have not yet shown both can be attained simultaneously. To examine this

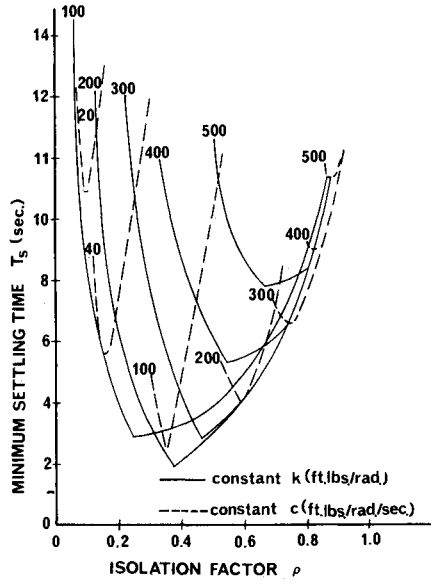

Fig. 9 Settling time vs isolation factor.

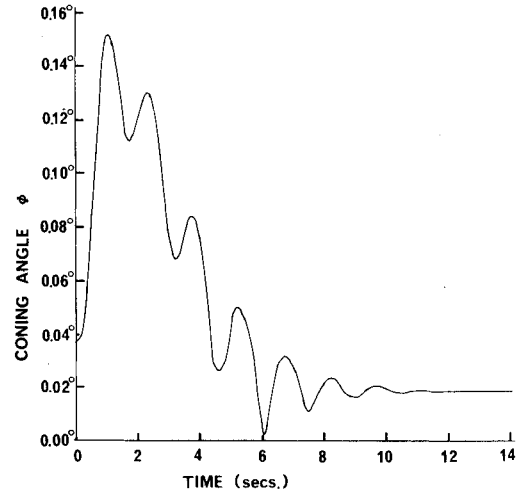

Fig. 10 Numerical integration of nonlinear equations.

question, we have calculated the isolation factor ρ for the system described by Eq. (29) with k and c taken as 200 ft-lb/rad and 124 ft-lb/rad/sec, respectively; these values minimize the settling time as shown in Fig. 4. The isolation factor for this case was 0.42, and this point is indicated by an asterisk in Fig. 8. Thus, even spring and damping constants selected specifically to minimize the settling time can provide a moderate degree of vibration isolation.

Next, isolation factors and settling times were calculated while k and c were allowed to take on values both larger and smaller than those providing the optimum settling time (k ranged from 100 to 500 ft-lb/rad, and c from 20 to 500 ft-lb/rad/sec.) The results of these calculations are summarized in Fig. 9 where along solid curves k remains constant while c varies, and along dashed curves c remains constant while k varies. These curves demonstrate the existence of a range of values of c and k over which settling times may be kept on the order of a few seconds with isolation factors substantially less than one. It thus appears that both of the desired performance goals may be attained simultaneously with a considerable degree of success.

Finally, because the results described in this paper have been based primarily on equations linearized not only in smal-variables, but also in small constants representing rotor unbalances, the full nonlinear equations of motion were programed on a digital computer to provide a means of verification. Figure 10 shows coning angle Φ vs time for one case. The system parameters were selected in accordance with Eq. (29), and k and c were 200 ft-lb/rad and 124 ft-lb/rad/sec, respectively. From the approximate linear relationships developed in the paper, the predicted settling time was 1.65 sec, and the predicted amplitude of steady-state coning motion was 0.0189° representing an isolation factor of 0.423. (These values are in accordance with Figs. 4 and 8.) Based on the computer output used to construct Fig. 10 it was determined that the predicted amplitude of steady-state coning was accurate to within 0.1%. Because of the difficulty of directly measuring settling time from this output, a curve-fitting process was required to check the accuracy of settling time predictions; the predictions agreed with the numerical integration results to within 2%.

References

[1] Landon, V. D., and Stewart, B., "Nutational Stability of an Axisymmetric Body Containing a Rotor," *Journal of Spacecraft and Rockets*, Vol. 1, No. 6, Nov.–Dec. 1964, pp. 682–684.

[2] Likins, P. W., "Attitude Stability Criteria for Dual-Spin Spacecraft," *Journal of Spacecraft and Rockets*, Vol. 4, No. 12, Dec. 1967, pp. 1638–1643.

[3] Rubin, C. P., and Swanson, R. V., "Feasibility Study of the Isolated Gyrostat Spacecraft," Rept. SSD 70446R, Oct. 1967, Hughes Aircraft Co.

[4] Johnson, C. R., "Tacsat I Nutation Dynamics," AIAA Paper 70-455, Los Angeles, Calif., 1970; also *AIAA Progress in Aeronautics and Astronautics: Communications Satellites for the 70's; Technology*, Vol. 25, edited by Nathaniel C. Feldman and Charles M. Kelly, MIT Press, Cambridge, Mass., to be published.

[5] Cloutier, G. J., "Nutation Damper Design Principles for Dual-Spin Spacecraft," *Journal of the Astronautical Sciences*, Vol. XVI, No. 2, March–April 1969, pp. 79–87.